

**Modeling, Design and Performance Study of a Linear Fresnel Plant: Application in Sahelian Rural Areas**

**Sory DIARRA<sup>1</sup>, Souley FAYE<sup>1</sup>, Sidy Mactar SOKHNA<sup>1</sup>, Ousmane SOW<sup>1</sup>**

1 Laboratoire Eau-Energie-Environnement et Procédés Industriels, Université Cheikh Anta DIOP, Ecole Supérieure Polytechnique, Fann, Dakar, Senegal

**ABSTRACT:** The aim of this work is to study a Linear Fresnel Plant (LFP) in rural Sahelian areas. An analytical method is used to model optical transfers in the system, followed by a sizing using MATLAB software. Then, the analytical method is compared with the Monte Carlo method using TONATIUH rays trace software. And finally, the optical characteristics of the LFP over the period from December to April are studied by simulation using TONATIUH. The design gives for a thermal power of 51.01 kW an opening area of the LFP field equal to 109.04 m<sup>2</sup> with a coverage rate of 75.41%. The comparison of the analytical method with that of ray tracing confirms the validity of the analytical method for the calculation of power. As expected, numerical simulations show for each day a peak of the power received around 13 h, and optical efficiency of the field increase from December to April.

**KEYWORDS:** Concentrated solar thermal collector, Linear Fresnel reflectors, Solar ray concentration, Thermal transfers, Mathematical modeling, Sizing, Simulations.

## 1 INTRODUCTION

In countries of sub-Saharan Africa only about 32% of the population have access to energy, among people having no access to electricity, 80% live in rural areas [1]. These regions are generally very sunny which makes solar technologies, in particular solar concentrators, very good alternatives for energy production. Among the solar-concentrating technologies, the most suitable for these mostly poor areas, are the Fresnel Linear Reflectors (LFRs). These are simple to design, affordable and can achieve the performance of parabolic trough concentrators [2] [3]. LFRs are relatively low cost compared to other solar concentrators [4]. However, little work of this type of concentrator has been carried out in this area. LFRs have not been studied much in the past, which explains the lack of mastery and the slow technological development of the system [5]. Our main objective is to perform the modeling, sizing and numerical analysis of a Linear Fresnel Plant for geographic coordinates 14.7° North and 17.4° West of Dakar, Senegal. It is important to choose the right software or tool according to the desired end result [6]. In our case, we used an analytical convolution method for sizing and a ray tracing method for the performance study. Mathematical modeling using the convolution method takes into account the reduction of optical losses by blocking and shading of the field which can greatly impact the efficiency of the system [7].

## 2 MODELING OF THE LINEAR FRESNEL PLANT (LFP)

For our study we have chosen a single pipe LFR thermal collector without a secondary concentrator. The decision not to use a secondary concentrator is justified by the fact that we are only interested in the field at the moment.

### 2.1 DESCRIPTION OF THE LINEAR FRESNEL PLANT (LFP)

The LFP consists of a field of flat plate reflectors of equal widths arranged in a row, and a monotube receiver with a glass tube to cover it and reduce heat losses by radiation (Figure 1 and Figure 2).

The reflectors are equipped with a system to track the sun around a single axis at an hourly angle. They are also long enough to observe the focal spot on the receiver without edge effects. To compensate for the cosine effect, which causes the focal spot to move along the longitudinal axis of the sensor, the receiver is able to translate along this axis during the day and depending on the period.

The receiver assembly is positioned high on the concentrator's plane of symmetry and its axis of symmetry is parallel to the reflector's tracking axis. It consists of an absorber monotube with a selective coating that converts the incident radiation into thermal energy, covered by a larger diameter glass tube designed to limit heat loss. A heat transfer fluid circulates inside the absorber tube to recover the thermal energy.

Geometric characteristics of the system are : the number of reflectors on both sides of the receiver ( $k$ ), the length and width of reflectors ( $L$  and  $w$ ), the position of each reflector and the spacing between reflectors ( $s$ ), the height and length of the receiver ( $f$  and  $L_p$ ), the Outside diameters of the absorber tube and the glass tube. The main physical characteristics are the optical properties of reflectors and receiver elements, as well as the thermo-physical properties of the heat transfer fluid.

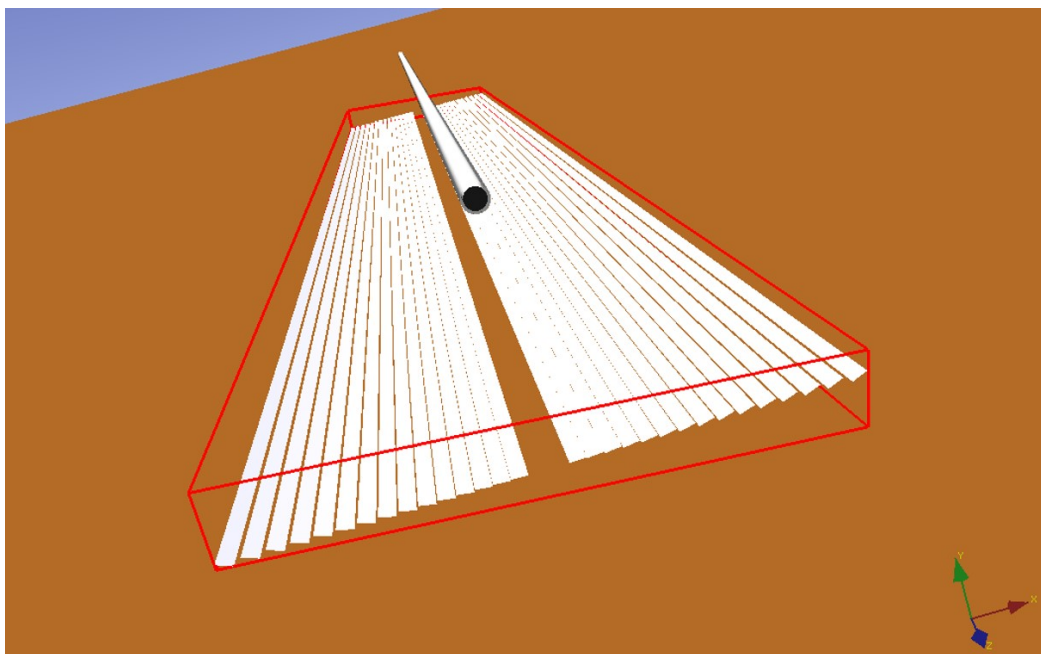


Fig. 1. LFR with tubular absorber

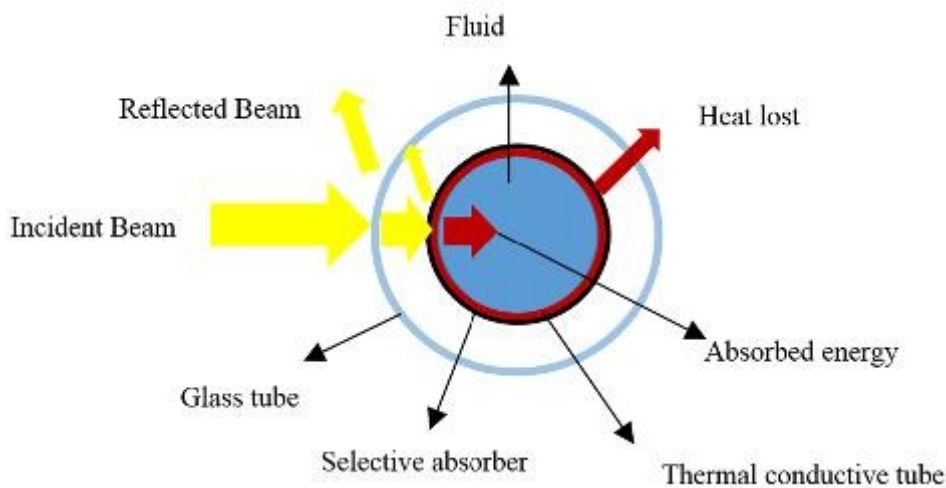


Fig. 2. Tubular receiver

## 2.2 GEOMETRIC PARAMETERS OF THE LFR SYSTEM

The geometry of the LFR thermal collector is mainly characterised by the width of the reflectors, their number, the height and the diameter of the absorber tube. Figure 3 and Table 1 give an exhaustive list of all these collector characteristics.

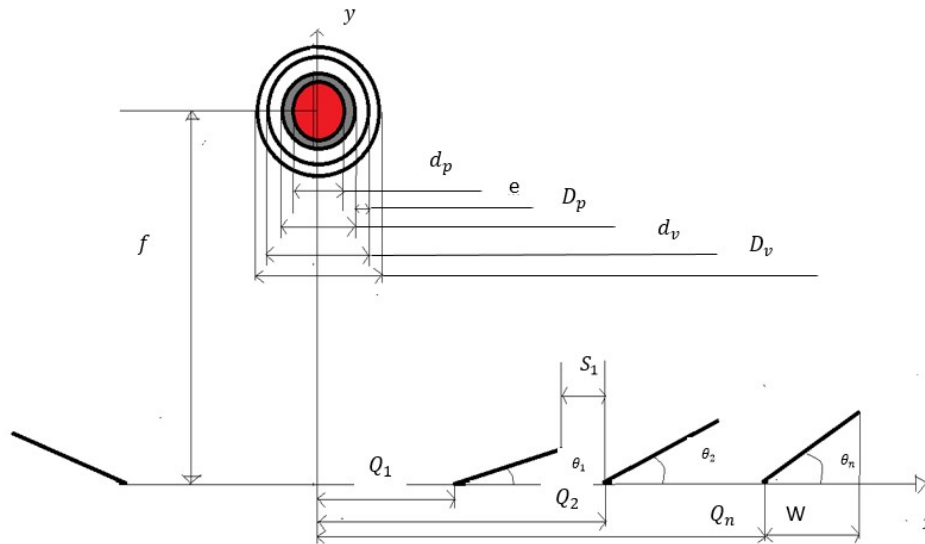


Fig. 3. Geometric characteristics of the LFR system

Table 1. Geometric characteristics of the LFR system

Parameter designation	Notation
Number of reflectors on either side of the receiver	$k$
Spacing between two reflectors	$S_n$
Reflector length	$L$
Width of reflectors	$W$
Reflector distance from vertical plane	$Q_n$
Tilt of a reflector relative to the horizontal axis containing the aperture plane	$\theta_n$
Height of the centre of the receiver from the plane containing the aperture surface	$f$
Length of the receiver	$L_p$
Internal diameter of the absorber tube (pipe)	$d_p$
External diameter of the absorber tube (pipe)	$D_p$
Inside diameter of glass tube	$d_v$
Outside diameter of glass tube	$D_v$
Width of the annular space between the absorber tube and the glass tube	$e$

### 2.3 MODELING RADIATIVE OPTICAL TRANSFERS

Our objective is to determine the total power received by the absorber tube and to be able to evaluate the optical efficiency. The analytical method developed by Mathur et al. [8] will be used. This method gives the position ( $Q$ ), inclination

( $\theta$ ) of each reflector and spacing (s) between the reflectors. It has the particularity, as illustrated in Figure 2, to avoid blocking and shading when the sun's rays have an incidence perpendicular to the plane containing the opening surface.

For a reflector "n" located on either side of the receiver ( $n = 1, 2, \dots, k$ ), the optical design gives its offset with respect to the center ( $Q_n$ ), its inclination ( $\theta_n$ ), its offset with respect to the reflector which precedes it ( $S_n$ ), the diameter of absorber tube needed to intercept all the reflected radiation ( $D_p$ ) and the total width of field ( $D$ ).

$$Q_n = Q_{n-1} + W \cos \theta_{n-1} + S_n \quad 1)$$

$$\theta_n = \frac{1}{2} \left[ \tan^{-1} \left( \frac{Q_n + \frac{W}{2} \cos \theta_n}{f - \frac{W}{2} \sin \theta_n} \right) \right] \quad 2)$$

$$S_n = W \sin \theta_{n-1} \tan(2\theta_n + \xi_0) \quad 3)$$

$$D_p = 2 \left[ W \sin \theta_k + \frac{Q_k + W \cos \theta_k}{\tan(2\theta_k - \xi_0)} - f \right] \sin(2\theta_k - \xi_0) \quad 4)$$

$$D = 2Q_1 + 2 \sum_{n=1}^k (W \cos \theta_n + S_n) \quad 5)$$

Once the solar rays are reflected, the appearance of several zones with different concentration ratios is observed on the surface of the absorber tube. Indeed, more a reflector moves away from the center, more its image on the surface of the absorber tube will be large. Therefore, the greatest concentration ratio will be at the center of the tube. For a number of reflectors on both sides of the receiver equal to "k", the number of zones on the surface of the tube will be "q = k + 1".

Each reflector (n) contributes to the surface of the tube. This contribution ( $CI_n$ ) is defined by [3] equal to:

$$CI_n = \frac{W \cos \theta_n}{r_n} \quad 6)$$

With ( $r_n$ ) the width of the image of reflector on absorber tube:

$$r_n = (\delta_{na} + \delta_{nb} + \delta_{nc}) \frac{D_p}{2} \quad 7)$$

Each area on surface of the absorber tube has its concentration ratio. The central part of the absorber tube which intercepts the contribution of all reflectors of the field has a local concentration ratio ( $LCR_1$ ) equal to [8]:

$$LCR_1 = 2 \sum_{n=1}^k CI_n \quad 8)$$

The local concentration ratio of the other zones of the absorber tube surface is given by:

$$LCR_i = \sum_{n=i-1}^{q-1} CI_n \quad 9)$$

With (i=2, ..., q)

To determine the power received by the absorber tube, we need in addition the surface of each zone. Thus, the area of the central zone 1 noted ( $C_1$ ) is given by:

$$C_1 = 2 * \delta_{a1} * \frac{D_p}{2} * L_p \quad 10)$$

The area of the second zone with the second largest concentration ratio ( $C_2$ ) is given by:

$$C_2 = 2 \left( \frac{\pi}{2} + \delta_{c1} - \delta_{a1} \right) \frac{D_p}{2} * L_p \quad 11)$$

From the third zone, the surfaces ( $C_i$ ) are given by:

$$C_i = 2(\delta_{c(i-1)} - \delta_{c(i-2)}) \frac{D_p}{2} * L_p \quad 12)$$

With (i=3, ..., q)

The absorbed radiation ( $\emptyset$ ) from the reflectors per unit aperture area ( $A_c$ ) is given by [4]

$$\emptyset = I_b \rho_r \alpha_p \gamma \tau_g \tag{13}$$

$I_b$ : The Direct Normal Irradiance of site (DNI)

$\rho_r$ : The specular reflectance of reflectors

$\tau_g$ : Glass cover transmittance

$\alpha_p$ : Absorber absorptance

$\gamma$ : The intercept factor

And the aperture area is equal to:

$$A_c = 2L \sum_{n=1}^k (W \cos \theta_n) \tag{14}$$

Thus, the flux density of each zone ( $\emptyset_i$ ) is given by:

$$\emptyset_i = \emptyset * LCR_i \tag{15}$$

With (i=1, ..., q)

Finally, the total solar power received by the absorber tube ( $P_p$ ) is given by:

$$P_p = \sum_{i=1}^q \emptyset_i C_i + I_b \tau_g \pi \frac{D_p^2}{2} L_p \tag{16}$$

The optical efficiency ( $\eta_0$ ) and the intercept factor ( $\gamma$ ) are given by:

$$\eta_0 = \frac{P_p}{A * I_b} \tag{17}$$

$$\gamma = \frac{P_p}{A_c I_b} \tag{18}$$

With  $A$  the total area of the field equal to:

$$A = D \times L \tag{19}$$

#### 2.4 MODELING OF THERMAL TRANSFERS WITHIN THE RECEIVER

In this part, our objective is to determine the thermal power lost by the receiver and the useful thermal power. The power lost by the receiver ( $Q_{Loss}$ ) can be determined by iteration from its three expressions [9]:

$$Q_{Loss} = \frac{2\pi\lambda_{eff}L_p}{\ln\left(\frac{D_p}{d_g}\right)} (T_p - T_{gi}) + \frac{\pi D_r L_r \sigma (T_p^4 - T_{gi}^4)}{\frac{1}{\varepsilon_p} + \frac{1 - \varepsilon_g}{\varepsilon_g} \left(\frac{D_p}{d_g}\right)} \tag{20}$$

$$P_{Loss} = \frac{2\pi\lambda_c L_p (T_{gi} - T_{ge})}{\ln\left(\frac{D_g}{d_g}\right)} \tag{21}$$

$$Q_{Loss} = \pi D_g L_p h_a (T_{go} - T_a) + \varepsilon_g \pi D_g L_p \sigma (T_{go}^4 - T_{sky}^4) \tag{22}$$

where the subscript p represents the absorber tube and subscripts a, gi and go represent the external environment, the glass inside and the glass outside. The cover thermal conductivity is  $k_c$  and  $k_{eff}$  is an effective conductivity for convection between the receiver.

In the same way, the useful power recovered by the fluid ( $Q_u$ ) is given by [9]:

$$Q_u = E [P_p - A_p U_L (T_{fi} - T_a)] \quad (23)$$

With E the Flow Factor

$$E = \frac{\dot{m} C_p}{A_p U_L} \left[ 1 - \exp \left( - \frac{A_p U_L F'}{\dot{m} C_p} \right) \right] \quad (24)$$

$U_L$  the Thermal Loss Coefficient

$$U_L = \frac{P_{Loss}}{A_p (T_p - T_a)} \quad (25)$$

And  $F'$  the Collector Efficiency Factor

$$F' = \frac{\frac{1}{U_L}}{\frac{1}{U_L} + \frac{D_p}{h_f d_p} + \frac{D_p \ln \left( \frac{D_p}{d_p} \right)}{2 \lambda_p}} \quad (26)$$

where the subscript  $h_f$  represents the convective heat exchange coefficient of the fluid.

### 3 SIZING OF THE LFP

The sizing of the LFP ensures the operation of a 3  $kW_e$  micro-ORC plant studied by Bouhamadi [10]. The necessary thermal power is 51  $kW_{th}$  and is capable of being obtained by LFR technology [11]. The sizing is carried out for the locality of Dakar with annual average climate data. A number of parameters has been set as shown in table 1. These choices are justified by studies that have been carried out. Singh [12] found that the optimal width of the reflectors (W) should be between 10 and 12 cm for better fixation and manipulation and the number of reflectors on both sides of the receiver (k) between 10 and 15 to have optimal overall performance. Xiao [13] shows that for latitudes less than 25 °, an orientation of north-south Tracking axis offers better efficiency. Finally, Duffie and Beckman[9] recommends a spacing between the absorber tube and the glass tube between 10 mm and 15 mm to minimize the thermal losses of the receiver. In addition, water was chosen as a thermal fluid.

**Table 2. Geometrical parameters fixed for sizing**

Parameter	Value
Number of reflectors	30
Width of reflectors	12 cm
Width of the annular space between the absorber tube and the glass tube	15 mm
Orientation of tracking axis	North-South

Sizing consists of determining the total area of the field and its geometric characteristics. The sizing methodology is presented in the form of the algorithm in figure 4. The methodology is first to fix all the input parameters such as the length of the reflectors and the receiver, the number of reflectors and the thermo-physical properties of the different constituting elements of the LFP. From this data, the geometric characteristics of the LFP are calculated such as the positions, inclinations and spacings of the reflectors and the diameters of the absorber tubes and the glass cover. The thermal power received by the absorber tube, the useful power recovered by the thermal fluid and the thermal losses of the receiver are then calculated. Finally, a comparison is made to check if the calculated thermal power output is equal to the one desired. If this is the case, the algorithm ends. Otherwise, the length of the reflectors from that of the receiver is increased and the calculations are resumed.

Since the equations of the model are almost all interdependent, they can only be solved iteratively. To solve the algorithm, a MATLAB program was written and the sizing results are presented in table 2.

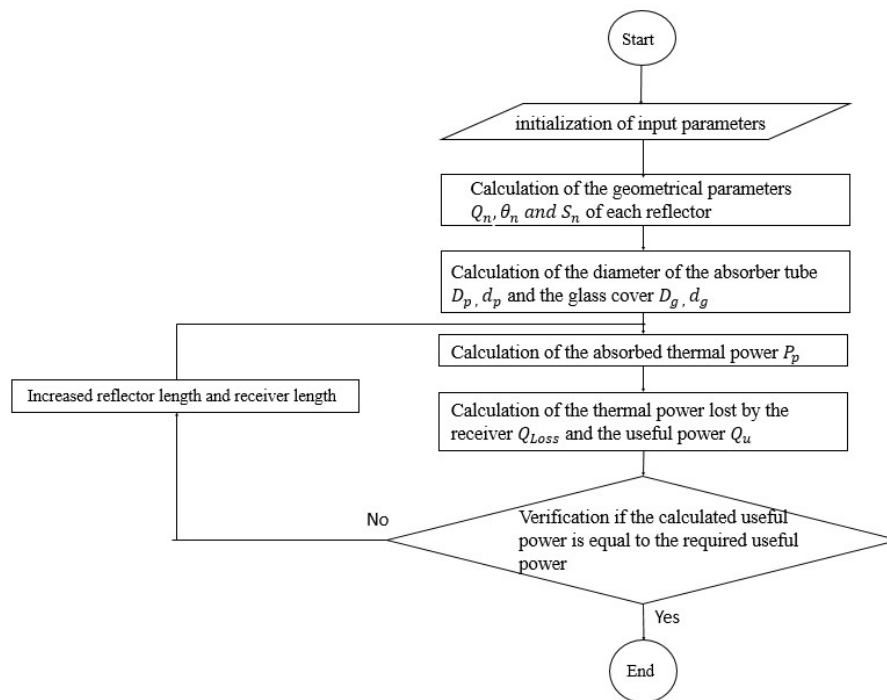


Fig. 4. Sizing methodology

Table 3. Sizing results

Parameter	Value
LFP field total area	109.64 m <sup>2</sup>
LFP field aperture area	82.68 m <sup>2</sup>
Coverage rate	75.41 %
LFP field width	3.44 m
LFP field length	24.023 m
Receiver height	1.82 m
Outside diameter of the absorber tube	0.1431 m

#### 4 COMPARISON OF THE ANALYTICAL METHOD AND THE MONTE CARLO RAY TRACING METHOD

In this part, the dimensioned LFP is modeled in the Tonatiuh rays tracing software to perform a flux map analysis on the absorber tube and determine the power received by the absorber tube (Figure 5). These results are compared with those obtained by the analytical method using MATLAB software.

Figure 6 represents the distribution of the incident flux on the surface of the absorber tube obtained by the Monte Carlo rays tracing method and Figure 7, the one obtained by the analytical method. The concentration profiles on the tube obtained are in good agreement with those opted for in the literature and follow the curve of the sun [14].

The analyzes show that the fluxes of different zones are more important with the Monte Carlo method than with the analytical method. However, the surfaces of different zones on the surface of the absorber tube are larger with the analytical method than with the Monte Carlo method. Knowing that the Monte Carlo method is the most accurate, the conclusion is that the analytical method tends to overestimate the area of the zones and to minimize their flux. On the other hand, the

total powers that reach the absorber tube are quite close with a relative error of 4%. This is explained by the fact that the two errors made with the analytical method is compensated when it comes to calculating the power received by the absorber tube. This analysis shows that the analytical method can be used for the calculation of powers.

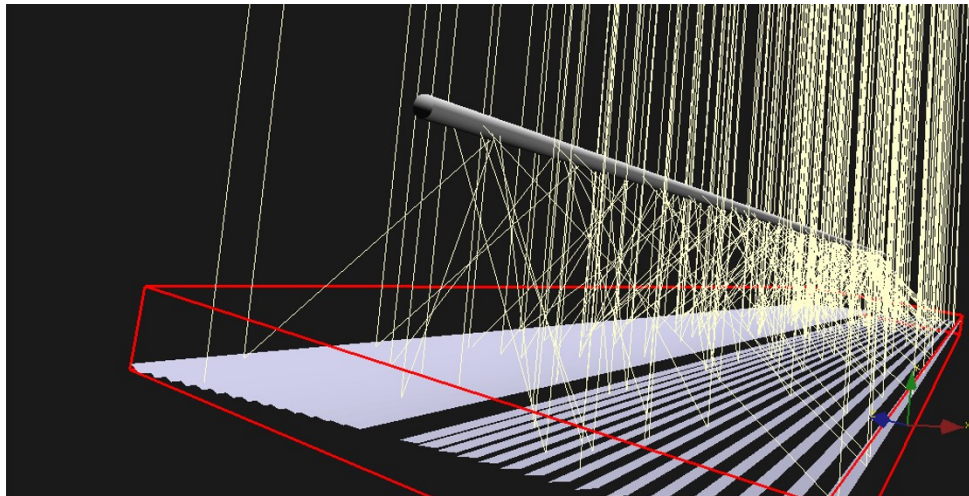


Fig. 5. Modelling the LFR concentrator on Tonatiuh

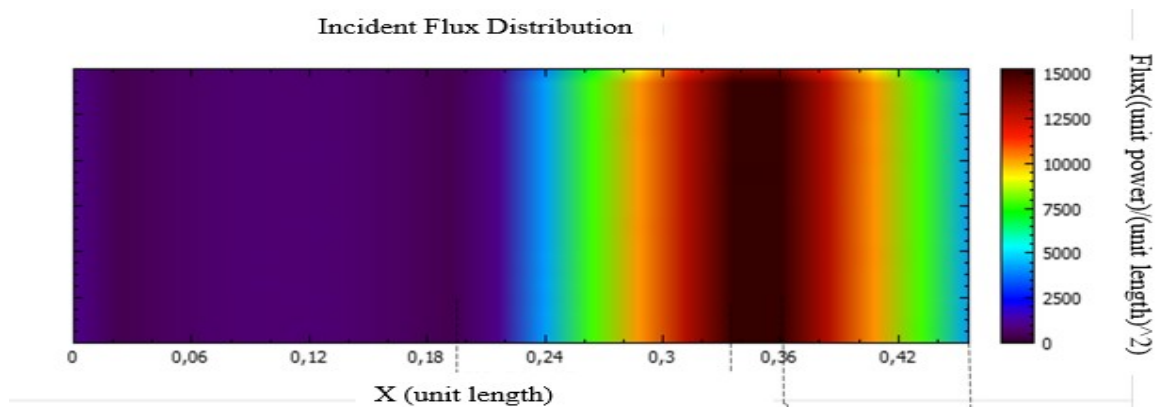


Fig. 6. Distribution of the incident flux on the absorber tube surface obtained by the Monte Carlo rays tracing method with TONATIUH

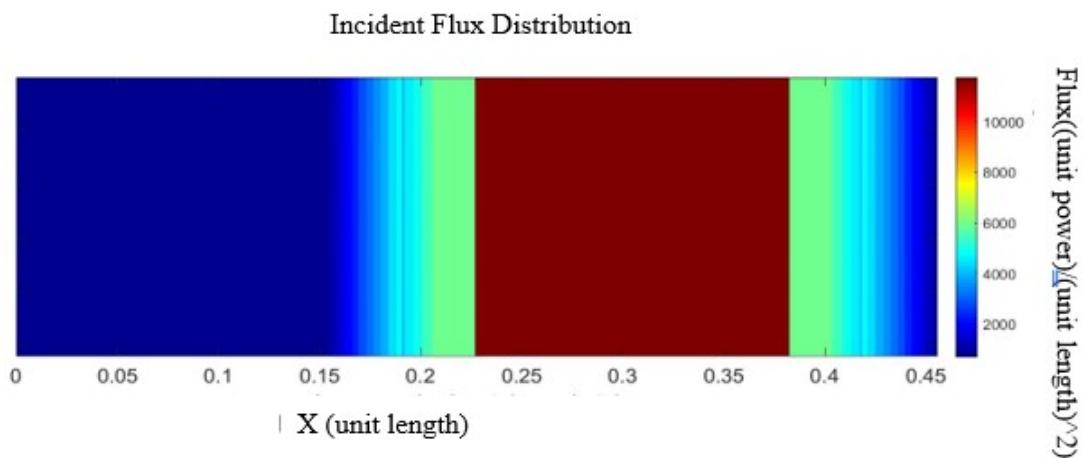


Fig. 7. Distribution of the incident flux on the surface of the absorber tube obtained by the analytical method with MATLAB



## 5 NUMERICAL STUDY OF LFP BEHAVIOUR ON DIFFERENT DAYS OF THE YEAR

### 5.1 METHODOLOGY

In this part, the LFP is simulated for the geographical coordinates of Dakar with the Tonatiuh software. Actual measured data of the DNI was collected and only over the period from December to April. Therefore, the simulations are run only during this period. Four specific days are chosen in this period namely December 28th, February 1st, March 22nd and April 5th. The simulations are run using time steps of 15 minutes. To avoid losses by cosine effect, the receiver is moved longitudinally with respect to its axis of symmetry. The data determined for each simulation point are the power received by the absorber tube, the power incident on the field, the thermal power recovered by the thermal fluid and the optical efficiency.

### 5.2 RESULTS AND DISCUSSIONS

Figure 8 shows that the power received by the absorber tube follows globally the variations of the incident power on the field, with the day of February 1st, which gives the highest powers. Each day a peak of power received by the absorber tube is observed around 13 h. This phenomenon is very characteristic of LFPs, which always give a peak of production in the middle of the day compared to a parabolic trough [15]. Indeed, this moment corresponds to the instant when the sun is the highest in the sky and the optical losses by shading and blocking are lower.

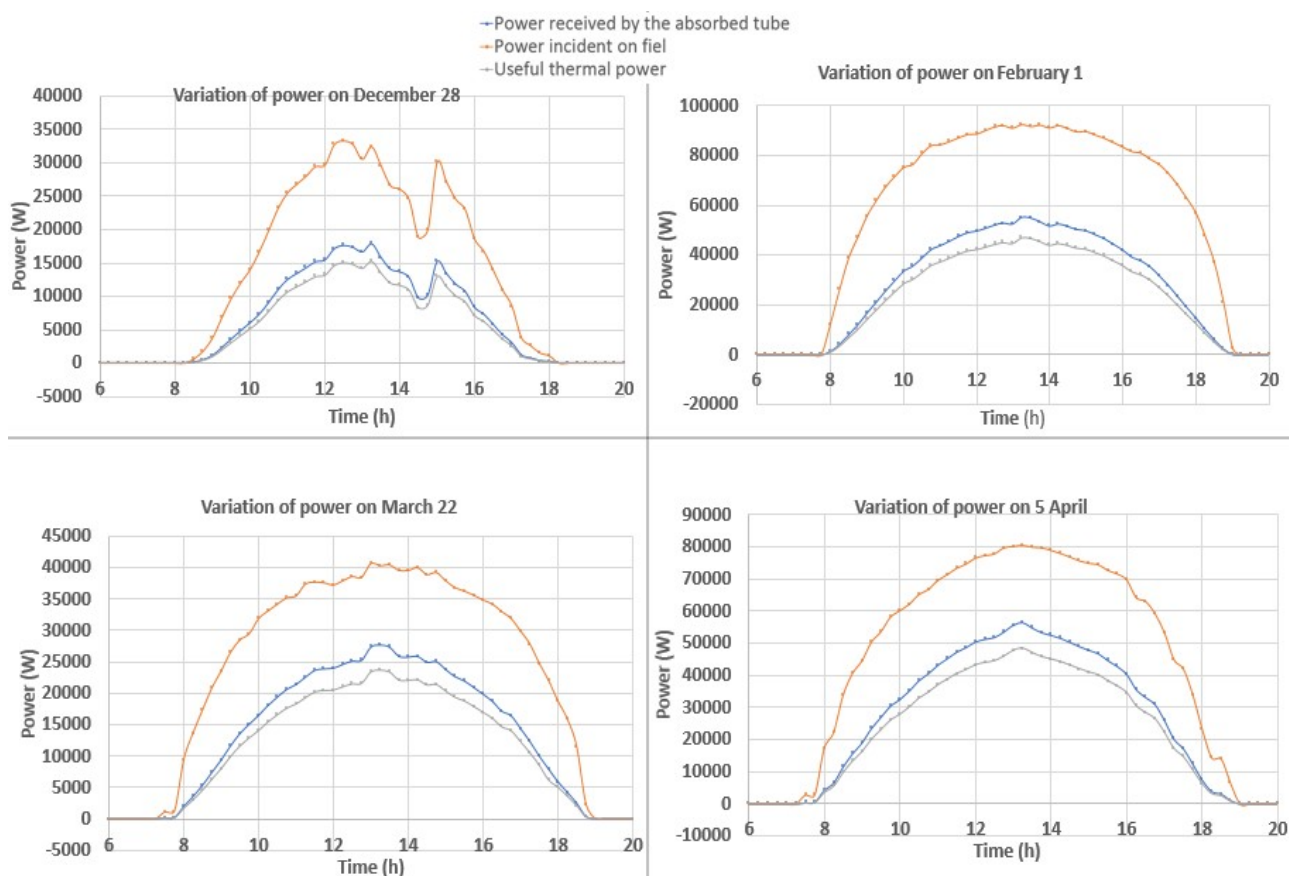


Fig. 8. Powers obtained for simulation days

Figure 9 shows the variations of optical efficiency. This efficiency increases day by day over the period from December to April, with always the peak around 13 h. This phenomenon is also explained by the fact that during the period from December to April for the geographical coordinates of Dakar, the height of the sun increases day by day. The higher the sun is in the sky, the less optical losses will be important. This shows the dependence of optical performance of the LFP with the height of the sun. We can also note that the optical yields obtained are consistent with the experimental tests carried out in the literature [16].

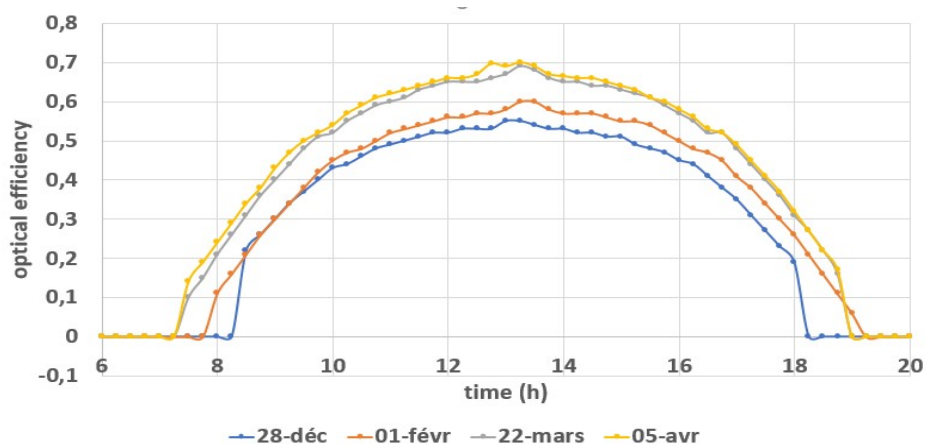


Fig. 7. Variation of the optical efficiency of the field during simulation days

## 6 CONCLUSION

In this work, an LFP was modeled and simulated for the city of Dakar Senegal with geographic coordinates 14.7° North and 17.4° West. The modeling was carried out using an analytical method. This method was compared to the ray tracing method, showing that it can be used for the calculation of the powers. The results of the simulations showed that the optical performance of the LFP is very dependent on the height of the sun. This means that a better field orientation, a more adequate tracking system, and optimized geometry could greatly improve the performance of the LFP. In our future works, the focus will be placed on the optimization and the realization of a prototype for the Sahelian rural areas.

## ACKNOWLEDGMENT

We would like to thank Ababacar Thiam and Césaire Ndiaye for giving us this opportunity to deepen our knowledge in this field. We are all grateful to him.

## REFERENCES

- [1] A. Thiam, E. I. Cissé, B. A. Ndiogou, K. Faye and M. Faye, "Design and CFD modeling of a solar micro gas turbine for rural zones areas," International SolarPACES Symposium, 2018, AIP Conference Proceedings 2126, 140006 (2019).
- [2] F. Veynandt, "Cogénération héliothermodynamique avec concentrateur linéaire de Fresnel : Modélisation de l'ensemble du procédé," Ph.D. thesis, Toulouse University, 2011.
- [3] Najla El Gharbia, b., Derbalb, H., Bouaichaouia, S., & Saida, N. (2011). A comparative study between parabolic trough collector and linear Fresnel reflector technologies. Energy Procedia 6 , 565–572.
- [4] MILLS, D. R., & MORRISON, G. L. (2000). COMPACT LINEAR FRESNEL REFLECTOR SOLAR THERMAL POWERPLANTS. Solar Energy Vol. 68, 263–283.
- [5] Abbas, R., Muñoz-Antón, J., Valdés, M., & Martínez-Val, J. (2013). High concentration linear Fresnel reflectors. Energy Conversion and Management 72, 60–68
- [6] Garcia, P., Ferriere, A., & Bezian, J.-J. (2008). Codes for solar flux calculation dedicated to central receiver system applications: A comparative review. Solar Energy, 189–197.
- [7] Moghimi, M., Craig, K., & Meyer, J. (2015). Optimization of a trapezoidal cavity absorber for the Linear Fresnel Reflector. Solar Energy 119 , 343–361.
- [8] S. S. Mathur, T. C. Kandpal and B. S. Negit, "Optical design and concentration characteristics of Linear Fresnel Reflector Solar Concentrators-II. Mirror elements of equal width," Energy Conversion and Management 31 (1991), pp .221–232.
- [9] J. A. Duffie and W. A. Beckman, "Solar Engineering of Thermal Process," Second, John Wiley and Sons, New York, USA, 1991.
- [10] S. Bouhamadi, "Evaluation du potentiel de la technologie solaire thermodynamique à concentration en climat désertique et sahélien : Cas de la Mauritanie," Ph D thesis, Dakar Cheikh Anta Diop University, 2017.

- [11] Bellos, E., Mathioulakis, E., Tzivanidis, C., & Belessiotis, V. ( 2016 ). Experimental and numerical investigation of a linear Fresnel solar collector with flat plate receiver. *Energy Conversion and Management* 130, 44–59.
- [12] G. Singh, “Technical note: Performance study of a linear Fresnel concentrating solar device,” *Renewable Energy* 18 (1999), pp .409-416.
- [13] G. Xiao, “Tilting mirror strips in a linear Fresnel reflector,” 2012, hal-00675222
- [14] Yu Qiu, Y.-L. H., & Ze-Dong Cheng, K. W. (2015). Study on optical and thermal performance of a linear Fresnel solar reflector using molten salt as HTF with MCRT and FVM methods. *Applied Energy* 146 , 162–173.
- [15] J. Dersch, G. Morin, M. Eck, A. Haberle “Comparison of Linear Fresnel and Parabolic Trough collector systems- System analysis to determine break even cost of Linear Fresnel Collectors,” *International SolarPACES Symposium*, 2009.
- [16] Mokhtar, G., BoumeddaneBoussad, & SaidNoureddine. (2016). A linear Fresnel reflector as a solar system for heating water : Theoretical and experimental study. *Case Studies inTherma lEngineering* 8, 176–186